



DYNA

ISSN: 0012-7353

Universidad Nacional de Colombia

Reyes-Mojena, Miguel Ángel; Sánchez-Orozco, Mario; Carvajal-Fals, Hipólito; Sagaró-Zamora, Roberto; Camello-Lima, Carlos Roberto  
A comparative study on slurry erosion behavior of HVOF sprayed coatings  
DYNA, vol. 84, no. 202, 2017, July-September, pp. 239-246  
Universidad Nacional de Colombia

DOI: <https://doi.org/10.15446/dyna.v84n202.56542>

Available in: <https://www.redalyc.org/articulo.oa?id=49655539027>

- How to cite
- Complete issue
- More information about this article
- Journal's webpage in redalyc.org

UNEN 

Scientific Information System Redalyc  
Network of Scientific Journals from Latin America and the Caribbean, Spain and Portugal

Project academic non-profit, developed under the open access initiative

# A comparative study on slurry erosion behavior of HVOF sprayed coatings

Miguel Ángel Reyes-Mojena <sup>a</sup>, Mario Sánchez-Orozco <sup>a</sup>, Hipólito Carvajal-Fals <sup>a</sup>, Roberto Sagaró-Zamora <sup>a</sup>  
& Carlos Roberto Camello-Lima <sup>b</sup>

<sup>a</sup> Facultad de Ingeniería Mecánica, Universidad de Oriente, Santiago de Cuba, Cuba. miguel@uo.edu.cu

<sup>b</sup> Faculdade de Engenharia Mecânica e de Produção, Universidade Metodista de Piracicaba, Santa Bárbara d'Oeste, SP, Brasil. crclima@unimep.br

Received: March 28<sup>th</sup>, de 2016. Received in revised form: December 15<sup>th</sup>, 2016. Accepted: February 3<sup>rd</sup>, 2017

## Abstract

In actual work, slurry erosion behavior of three different HVOF sprayed cermet coatings has been studied. The coatings were developed using the powders feedstock having WC fine structured sizes, Cr<sub>3</sub>C<sub>2</sub>-NiCr 75-25 and NiCrWSiFeB, latter conventional grain sizes. The slurry erosion testing was performed using a laboratory made pot-type slurry erosion tester, at an impact velocity of 3.61 m/s and 9.33 m/s and impact angle of 30 and 90°. The mechanism of material removal in slurry erosion was studied and discussed on microstructural investigations and mechanical properties under the erosion conditions. It was observed that the WC-CoCr cermet coating with fine WC grain exhibits higher erosion resistance as compared to conventional cermet coating due to its improved properties like low porosity, high micro-hardness and fracture toughness.

**Keywords:** slurry erosion; nanostructured coatings; HVOF, thermal spray coatings.

# Estudio comparativo del desgaste en mezclas erosivas de recubrimientos depositados por HVOF

## Resumen

Este trabajo investiga el comportamiento del desgaste en mezclas erosivas de recubrimientos depositados mediante la técnica de proyección térmica usando el proceso HVOF. Se analizaron tres tipos de recubrimientos, WC-CoCr con estructura de grano fino, Cr<sub>3</sub>C<sub>2</sub>-NiCr 75-25 y NiCrWSiFeB, estos últimos con tamaños de grano convencional. Los ensayos de desgaste erosivo se desarrollaron usando un tribómetro de recipiente de mezclas para evaluar la resistencia a la erosión de los recubrimientos a velocidades de impacto de 3.61 m/s y 9.33 m/s y ángulos de impacto de 30 y 90°. El mecanismo de desgaste de los recubrimientos fue estudiado y discutido sobre la base del examen microestructural y la influencia de sus propiedades mecánicas. Se observó que el recubrimiento de carburo de tungsteno exhibe mejor resistencia a la erosión comparada con los recubrimientos de carburo de cromo y metálico debido a sus propiedades de microdureza, tenacidad a la fractura y menor porosidad.

**Palabras clave:** desgaste en mezcla erosiva; recubrimientos nanoestructurados; HVOF; recubrimientos por proyección térmica.

## 1. Introduction

A common and unavoidable problem in industrial environments that constantly accompanies the operations of various mechanical components is wear that demands the development of new kind of materials with better properties for applications in those processes with severe conditions of wear, corrosive medium and exposed to high temperatures.

An alternative to solve these problems is the technique of thermal spraying which allows applying coatings of different natures, versatility and improve the properties of material surfaces, its properties and performance. This technique has gained popularity today because obtaining surfaces with exceptional properties such as: wear resistance, corrosion resistance, weight reduction and a relative low cost [1].

For industrial applications, cermets based coatings are

**How to cite:** Reyes Mojena, M.A., Sánchez Orozco, M., Carvajal Fals, H., Sagaró Zamora, R. and Camello Lima, C.R., A comparative study on slurry erosion behavior of HVOF sprayed coatings DYNA, 84(202), pp. 239-246, September, 2017.

widely used to modify the surface and improve the wear resistance of the mechanical components. Particularly successful and widely employed in different wear conditions are coatings WC-Co, however the feasibility of using these in certain corrosive and erosive-corrosive environments is debatable, compared with the new coatings of WC-CoCr [1,2], that create dense coatings with high hardness and good resistance to abrasion, erosion and erosion-corrosion. Slurry erosion resistance of WC-10Co-4Cr sprayed coated samples has improved by the addition nano WC-12Co powder into the coatings. However, the studies on slurry erosion of nanostructured are scarce in the literature. Based coatings CrC-NiCr systems, although usually shown lower hardness present greater stability with increasing temperature and have better corrosion resistance [3,4].

The main techniques used for the deposition are the plasma spraying air (APS) and the oxy-fuel flame at high speeds or hypersonic flame (HVOF). The HVOF technique is one of the most used method for the deposition of coatings of WC-Co and CrC-NiCr due to its unique characteristics such as high speed flow of particles to deposit and low temperature. This method causes less decomposition of WC during spraying compared to plasma spraying [5,6]. This deposition procedure has the ability to produce higher quality coatings as regards low porosity, oxide content, density and high hardness and wear resistant.

Therefore, the aims of this work is to study the behavior erosive wear of three types of coatings classified according to their grains sizes on nanostructured (WC-CoCr) and conventional and their chemical composition: coating of tungsten carbide (WC-CoCr), chromium carbide ( $\text{Cr}_2\text{C}_3$ -NiCr 7525) and Nickel based (88HV) metal coating, all of them deposited by HVOF.

## 2. Materials and Experimental procedures

### 2.1. Coating materials

The coatings were deposited onto a steel substrate of low carbon (AISI 1020), selected due to its great industrial applicability and relatively low cost. The substrate surface was polished and blasted with aluminum oxide in order to remove impurities and obtain adequate roughness on the surface to be coated. The coating was applied achieving an average value of thickness  $440 \pm 17 \mu\text{m}$  covering an area of  $75 \times 25 \times 3 \text{ mm}$ .

The substrates of AISI 1020 were coated through the technique called hypersonic High Velocity Oxy-Fuel / (HVOF). The commercially available feedstock materials were agglomerated and sintered with different particle sizes of the powders. One with a chemical composition related to a coating of tungsten carbide nanostructured (primary carbide size  $200\text{--}500 \text{ nm}$  approximately) WC-10Co4 Cr (1350 VM / WC-731-1 / Praxair, Concord, NH, USA with agglomerated particle size of  $-45 / +15 \mu\text{m}$ ), the other related to a chromium carbide coating of conventional structure ( $\text{Cr}_3\text{C}_2$ -NiCr 75-25 HC Starck Amperit® 588,074, with particle size  $45/15 \mu\text{m}$ ) and a metal compound NiCrWSiFeB coating (Colmonoy 88HV / Wall Colmonoy Corporation with particle size  $05/10 \mu\text{m}$ ). The chemical composition of these materials is shown on Table 1.

Table 1.

Nominal composition of coatings deposited by the HVOF method.

Materials	% Wt						
	C	W	Co	Cr	B	Ni	Si
1350	5,4	Bal	10,1	4,2	-	-	-
7525	11,0	-	-	Bal	-	19,0	-
88HV	0,8	16,5	-	15,0	3,0	Bal	4,0

Source: Authors

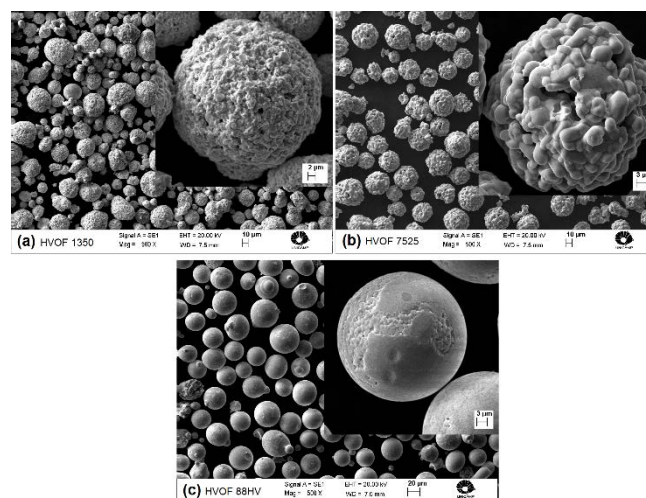


Figure 1. Images of scanning electron microscopy (SEM) micrograph of materials in powder form: (a) 1350 VM / WC-731-1, (b) Cr<sub>3</sub>C<sub>2</sub>-NiCr AMPERIT 75-25 and (c) Colmonoy 88HV; used as a deposit.

Source: Authors

Table 2.

Thermal spray process parameters.

Process parameters	Deposited coatings		
	1350	7525	88HV
Flow rate, O <sub>2</sub> (scfh)	1850	1950	2000
Flow rate, N <sub>2</sub> (scfh)	25	23	25
Flow rate (Kerosene)	6,0 GLP	5,5 GLP	6,0 GLP
Standoff distance (mm)	350÷400		

Source: Authors

Fig. 1 shows images of scanning electron microscopy micrograph of the powders used in the HVOF, the enlarged details of the images displayed agglomerated particles and sintered spherical morphology.

### 2.2. Thermal spray coating deposition

The technique used for thermal spraying was HPHVOF, High Pressure High Velocity Oxygen Fuel (JP- 5000, Praxair-Tafa, Concord, NH, USA). Spray application parameters used in the thermal spray process for each material were adjusted according to the recommendation of suppliers and are shown on Table 2.

### 2.3. Coating characterization

Coating microstructure was initially examined by both optical and scanning electron microscopy (SEM). of the top surfaces and cross-sections. Following all erosion tests the surface was examined using light and SEM to determine the

extent of degradation and to identify the material loss mechanisms.

Microhardness measurement was done with a Vickers indenter (SHIMADZU, model HMV-G). For microhardness testing, ten measurements were made on each sample in a horizontal line in the median plane of the cross section to minimize edge effects and interface with the substrate and a load of 0.3 kg was applied with a dwell time of 15 s.

Fracture toughness of the coatings was determined by indentation method at 2 kg load with 20 s dwell time. The indentations were taken at the coating cross-section and SEM images of these indentations were analyzed for studying the propagation of corner cracks and measurement of crack lengths. The fracture toughness (K<sub>IC</sub>) was evaluated using well-established formulations reported by other researchers [1,7].

Porosity analysis was done using the technique of SEM microscopy and image processing. The software used was the ImageJ 1.48V and images used for analysis were selected with increased 500X.

The surface roughness (Ra) value of as-sprayed coatings was measured by an optical roughness tester (MITUTOYO SURFTTEST 211)

#### 2.4. Experimental setup and erosion testing

The tribological properties of the coatings (erosive wear resistance) were measured using a pot type slurry erosion tribometer [1,8] (Fig. 2a). Coated samples were first ultrasonically cleaned in acetone and dried up until all the moisture was removed and weighted to 0.1 mg precision. Cleaning the samples it was also carried out after each erosive test in order to remove any of the eroded material. The specimens were disposed over the two circular plates, specially designed to evaluate particle impact angles ( $\alpha$ ) of 30 and 90° (Fig. 2b and 2c). The circular plates rotate with 660 and 1550 rpm with an instantaneous cylindrical velocity ( $v$ ) of 3.61 and 9.33 m/s respectively, at the tip of specimens. SiO<sub>2</sub>- 30/40 type (quartz sand) with grain size between 300 ÷ 425  $\mu$ m and hardness HV=1100, were used as erodent, mixed with fresh water in a concentration of 30% wt of abrasive particles (Fig. 2d). Erosion tests were performed for a maximum time of 6 hours at 1 hour intervals, in which mass loss of the samples tested, were determined to evaluate the performance of the coatings. Each test was replicated 3 times. Weight losses were measured and results are reported as the volume of material eroded per unit mass of erodent particles used during the tests. The results of mass losses were obtained by weight difference determined sample volume loss (W<sub>v</sub>) with the following expression:

$$W_v = \frac{W_g \times 1000}{\rho} \quad (1)$$

Where W<sub>v</sub> is the volume loss (mm<sup>3</sup>), W<sub>g</sub> accumulated mass loss (g) and  $\rho$  the density of the deposited material (g / cm<sup>3</sup>).

The results obtained from the experiments were statistically processed in order to show their statistical significance. For data processing professional Statgraphics Centurion XV software was used. All statistical analyzes present at this work were performed with a confidence level of 95%.

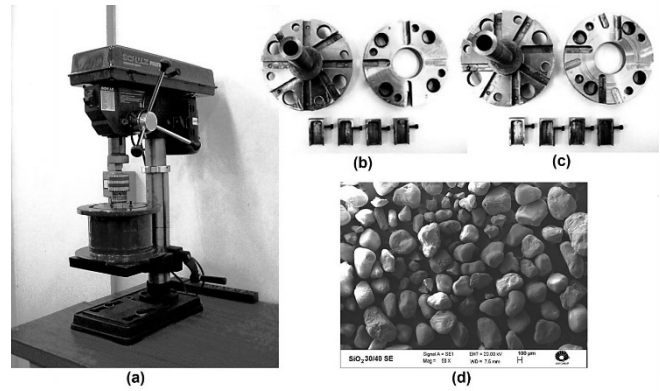


Figure 2. Experimental setup: (a) Pot type slurry erosion tribometer, (b and c) circular plates to fix samples ensuring angles impact of particles on the coatings 30 and 90°, (d) electron microscopy image (SEM) of quartz sand (SiO<sub>2</sub> - 30/40 SE) used as erodent particles.

Source: Authors

Table 3.

Mechanical properties of coatings

Coatings	Mechanical properties			
	Microhardness (HV <sub>0.3</sub> )	Toughness (K <sub>IC</sub> ) MPa m <sup>1/2</sup>	Porosity (%)	Roughness ( $\mu$ m)
1350	1201,6 ± 70,71	9,70 ± 1,55	0,39 ± 0,03	4,42 ± 0,32
7525	772,2 ± 66,812	7,35 ± 2,34	4,89 ± 0,69	5,51 ± 0,31
88HV	743,5 ± 21,50	6,70 ± 4,29	4,29 ± 1,50	5,97 ± 0,23

Source: Authors

### 3. Results and discussion

#### 3.1. Coating characterization.

Results of microhardness, toughness, porosity and roughness of coatings are shown on Table 3.

The microhardness values of the coatings tested are very similar to those found in the literature for coatings applied by HVOF [1,9,10] process and correspond to the values provided by the manufacturer.

It is also noted on Table 3 that the coating obtained with nanostructured powder (1350), presents the lowest values of roughness and porosity and higher values of microhardness and fracture toughness if these parameters is compared to those with the rest of the coatings tested (powders with conventional size), playing a key role the dimension the particle size of the powder [1,9-12].

#### 3.2. Microstructural examination

Fig. 3 shows the microstructures of the cross sections of coatings deposited by HVOF. According to the optical and SEM micrographs, there is good adhesion between the substrate and coatings.

SEM micrograph shown on Fig. 4a presents the microstructure of the material 1350 consisting of a dark phase related to the matrix (chrome cobalt) with a clear phase composed of reinforcing particles (WC) uniform distributed. SEM image in Fig. 4b shows the structure of the material Cr<sub>3</sub>C<sub>2</sub>-NiCr 75-25 AMPERIT composed of two clear phases related NiCr binder matrix and a darker linked to chromium

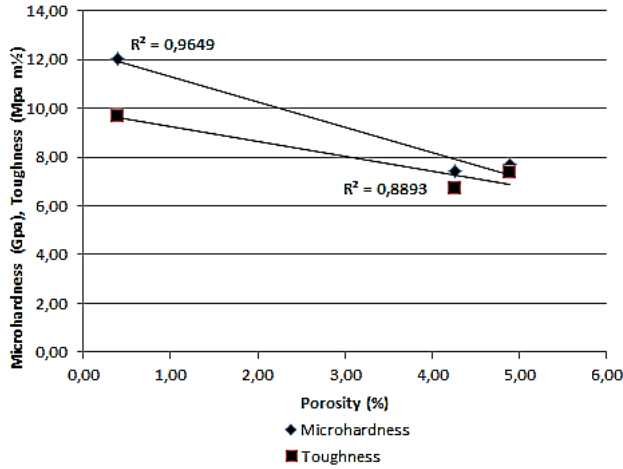


Figure 3. Relationship between porosity, micro-hardness and toughness of the materials on the analyzed deposits.

Source: Authors

carbides with a more macroscopically heterogeneous microstructure including irregular-shaped pores. Fig. 4c shows a microstructure of the 88HV coating shows a pronounced layered and heterogeneous microstructure at the macro level with regions of both phases where the WC particles may be observed in a matrix of nickel-chromium and borides of different nature, showing, moreover, a mixture of splats and incompletely melted precursor particles surrounded by irregular-shaped pores.

Images of Fig. 4 also show a more dense and homogeneous coating on tungsten carbide with more uniform particle reinforcement (WC) distribution microstructure for 1350 coating. By the other hand, SEM images are evidence of the presence of interlamellar defects such as pores and cracks, which are greater in the coatings shown in Fig. 4b and c.

### 3.3. Erosive wear test.

The results of the erosion experiments carried out for the different evaluated coatings are presented on Table 4 in form of erosion rate of each coating to facilitate comparison of materials with different densities. The effects of various factors influencing the results are analyzed below.

Fig. 5 shows the surface plots, where the influence of the angle and speed of impact factors of erosive particles in the dependent variable erosion rate (Er) is observed. From the analysis of this figure it can be observed that for impact velocities of particles of 3.61 m / s the value of the angle of impact does not have a great influence on the magnitude of the rate of erosion experienced by the coatings. However, when speed is higher (9.33 m / s), the highest values of the erosion rate of the coatings are related to the impact angle of 90 °, that defines this experimental condition as the critical one and this behavior is attributed to the fragile nature of the coatings and the kinetic energy present erosive particles when the impact velocity is greater [13-15].

For the test condition of minimum speed (V=3.61 m / s), erosive wear behavior of the coatings can be associated to the damping effect of the solid particles with the water present in

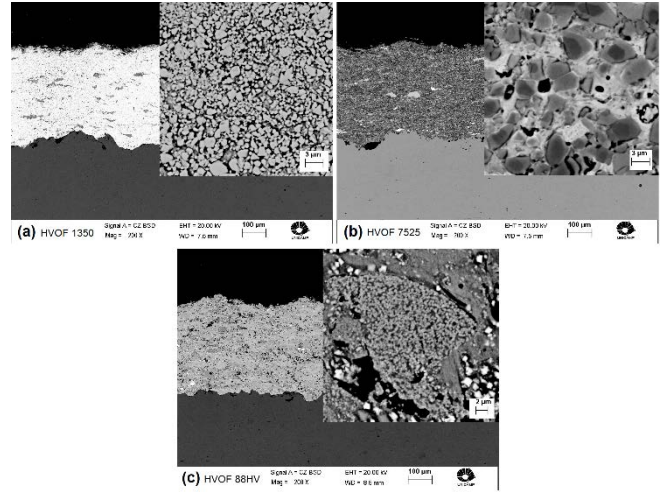


Figure 4. Images of scanning electron microscopy (SEM) of the e cross sections (a) 1350 VM / WC-731-1, (b) AMPERIT Cr3C2-NiCr 75-25 and (c) Colmonoy 88HV.

Source: Authors

Table 4.  
Rate of erosive wear, Er (mm³/Kg)

Coatings	Experimental Setup			
	$\alpha=30^\circ$	$\alpha=90^\circ$	$\alpha=30^\circ$	$\alpha=90^\circ$
	$v=3,61 \text{ m/s}$	$V=3,61 \text{ m/s}$	$v=9,33 \text{ m/s}$	$V=9,33 \text{ m/s}$
1350	2,823	2,125	8,397	9,353
7525	3,829	3,969	27,022	34,955
88HV	2,293	2,194	15,253	25,370

Source: Authors

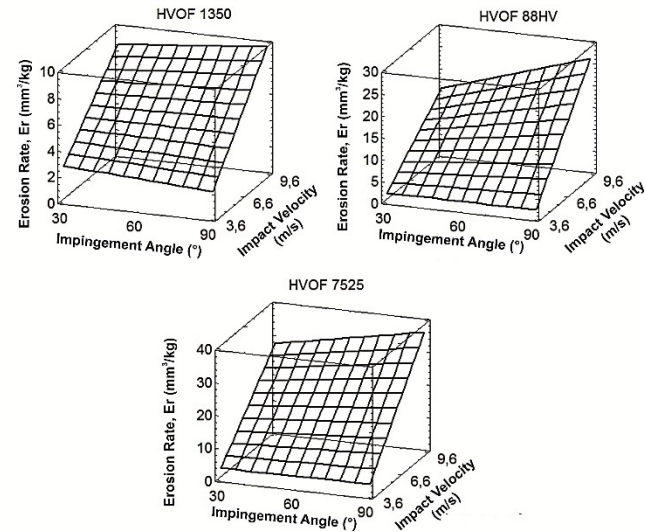


Figure 5. Erosion rates at two impingement angles and impact velocities fort each coatings.

Source: Authors

the mixture and the low kinetic energy that the solid product particles reach at this speed value [12]. When the impact velocity of the particles is increased is greater kinetic energy than those that they had and the greater energy dissipated by impacting the surface of the coatings, is used to remove the



unit volume of material eroded by the erosion mechanism [16,17]. The performance of all coatings suggests strongly that the impact speed is a parameter that has a great influence on the behavior of erosive wear coatings. Similar behaviors are reported in literature [13,18].

Fig. 6 corresponds to the analysis of variance of the mean values of erosion rate defined above experimental critical condition. From figure it can be observed that 1350 coating has the best performance in terms of erosion resistance (lower value of the erosion rate) with a great statistically significant relationship when compared to 88HV and 7525 coatings. However, these latest coatings form a homogeneous group where no statistically significant difference between them.

The higher hardness of the erodent particles is another factor that has a great influence in efficient cracks that are initiated in the target. The effect of the ratio of the target material hardness to erodent particle hardness ( $HVM/HVP$ ) seems to be decisive for both impingement angles, but only at the critical condition of  $v=9.33\text{ m/s}$ . In these conditions of high kinetic energy of abrasive particles a low cycle fatigue failure of the carbide matrix and large carbide grains and microcutting occur depending on the ratio of material as well as abrasive hardness.

If material hardness exceeds that of abrasive, like 1350 coating the more wear resistant coating; the erodent particles are not able to cause plastic flow in hard target and the wear comes from a low-cycle fatigue failure of the carbide matrix and carbide grains.

If the hardness of an abrasive exceeds that of coating (88HV, 7525 NiCr) the following processes take place: penetration of abrasive into the material surface, microcutting or plowing, failure of large carbide grains, resulting in the detachment of small chips.

As was previously noted, the erosion wear resistance of the coatings depends greatly on their fragile nature, playing an important role a number of factors including the kinetic energy of particles linked to the impact velocity, the particle size, the microhardness and fracture toughness of the eroded surface [19,7,20]. In opinion of the authors, wear nature mechanism

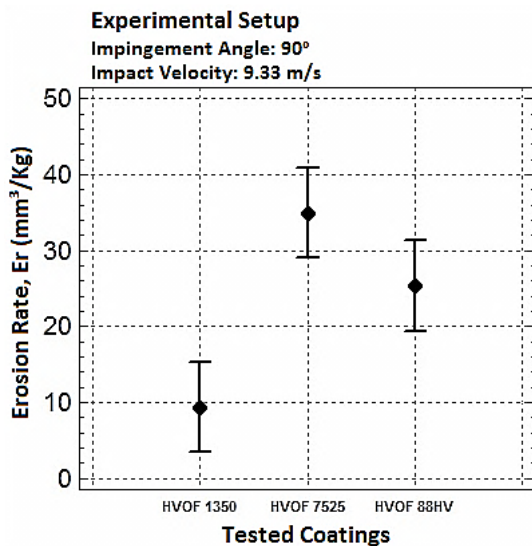


Figure 6. Analysis of variance for erosion rate under the critical condition.  
 Source: Authors

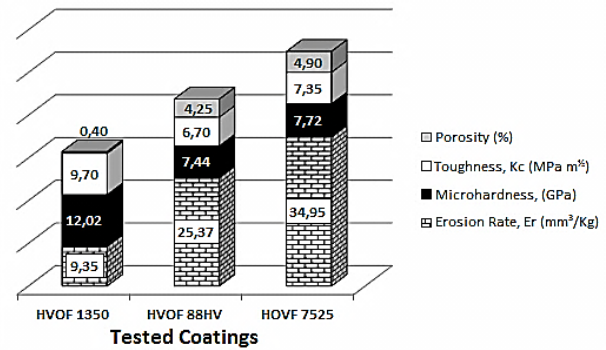


Figure 7. Erosion rate as a function of porosity level, fracture toughness and microhardness of HVOF coatings for critical condition.  
 Source: Authors

ultrafine and nanometrics cermets occurs due to a complex mechanism beyond a simple classification of ductile and brittle materials, that even does not apply equally to volumetric materials and coatings, beyond the effect on each mean grain size of the carbides and density of the deposit [17,7,21].

Some of these factors mentioned above and their relation to explain the behavior of the three coatings can be seen on Fig. 7. It can be observed that the level of porosity plays an important role in erosion wear resistance. When porosity is high (greater than 2 to 3%), the wear resistance can be significantly reduced due to the low adherence of carbide grains to the binder matrix, the low hardness and toughness of these coatings and during repeated impacts of erodent particles on a given area in the coating, the stress variation let crack forming and their propagation precisely in pores as starting point [14,15,23].

From Fig. 7, it can be observed that cemented carbide coating, WC-CoCr shown the best performance for the experimental critical conditions as a result of a more dense and homogeneous coating microstructure (Fig. 3), because of its greater microhardness, lower porosity and higher fracture toughness. Nanostructured coating samples is showing a moderate type of erosion effect as shown on Fig. 7. This proves that nanostructured coating gives satisfactory performance even in extreme wear conditions due to high hardness and fracture toughness.

Although there is no model to explain satisfactorily the behavior of the coating erosion rate formed by layers deposited by the technique of thermal spraying, some researchers included in such models two variables related to the mechanical properties of the deposited material: microhardness and fracture toughness [16-18,22,23]. Fig. 8 shows the correlation obtain by the authors in order to relate properties such as fracture toughness ( $Kc$  -  $\text{MPa m}^{1/2}$ ) and the microhardness of the coatings ( $Hv$  -  $\text{Kg/mm}^2$ ), with the erosion rate ( $Er$ ). The relationship between hardness ( $HV$ ) and fracture toughness ( $Kc$ ) plays a dominant role in controlling erosion mechanism of the coatings. As shown in Fig. 8, 1350 coating gives satisfactory performance even in extreme wear conditions due to high hardness and fracture toughness ensuring the lowest levels of erosive wear. Hardness and toughness of the coatings can be improved by

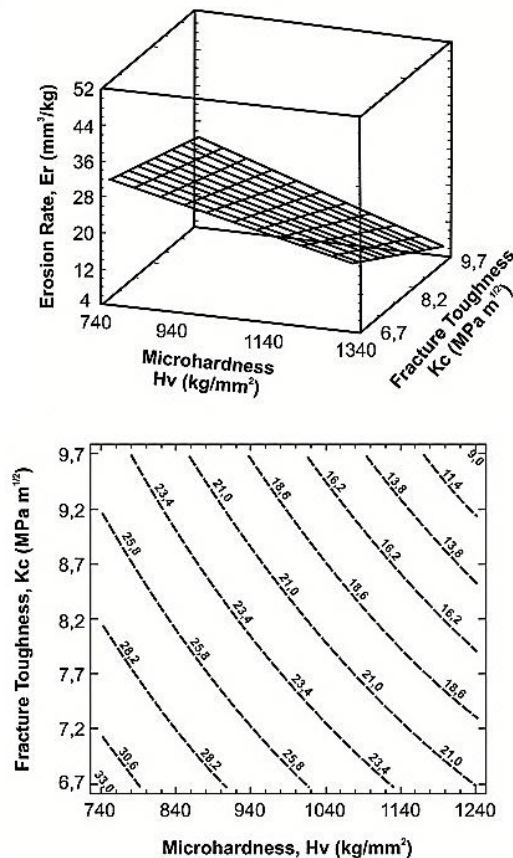


Figure 8. Correlation between erosion rate and microhardness as well as fracture toughness for analyzed coatings (a) Surface plot. (b) Contour plot  
Source: Authors

decreasing the WC grain size to near nanometer range that results in enhanced erosion resistance.

The behavior of this nanostructured coating suggests that it may be possible to increase the hardness and wear resistance of these materials still further without compromising toughness substantially.

Important decisions can be made from the behavior of wear rate of the tested coatings from the aforementioned relationship between hardness and toughness of the material, aspects very controversial because generally increased hardness means a substantial decrease in fracture toughness. Fig. 8 presents the relative ranking of the coatings investigated with respect to erosion rate and could be explained in opinion of authors of the present study, by their different fracture toughness values whereas the hardness seems to be of minor importance.

As shown in the above figure, greater wear resistance coating corresponds to higher microhardness and fracture toughness (nanostructured). Such behavior suggests a major role of fracture toughness more than the microhardness of the material.

However in the analysis of the figure the role related to relationship between hardness of the abrasive particle and target must be considered. Figure for example can be seen that hardness below 1100 HV, the wear of materials increases drastically. Beyond and with the highest fracture toughness

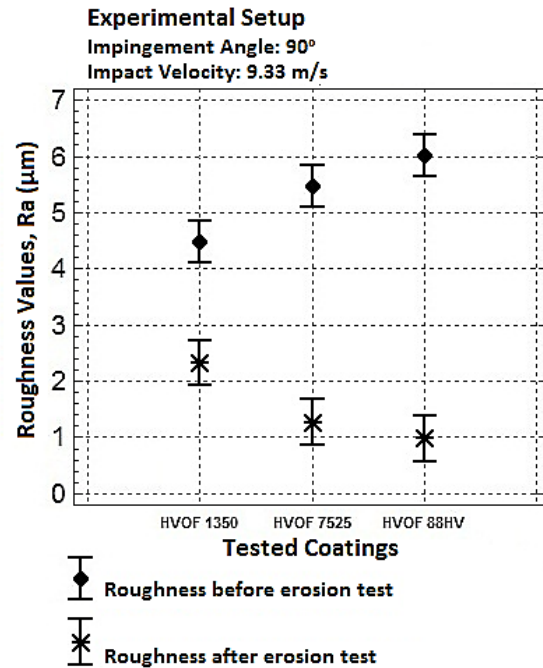


Figure 9. Variance analysis of mean values of the roughness of coatings before and after erosion test.  
Source: Authors

values, greater resistance to wear is achieved by tested materials (Fig. 8a).

Fig. 8b shows a contour plot that illustrates the best combination to obtain a significant wear resistance by achieving a hardness between 1170-1240 HV and a fracture toughness,  $k_c = 9-9.7 \text{ MPa m}^{1/2}$ .

Another factor used in the characterization of surface coatings was roughness. Determined before and after erosion tests (initial roughness values of the coatings shown on Table 3) the values obtained after eroding surfaces with a statistical analysis of variance can be observed on Fig. 9.

Fig. 9 shows clearly two homogeneous groups, one formed by coating tungsten carbide (1350) and another by the chromium carbide coating and the metallic coating (7525 and 88HV). Between the two groups there is a statistically significant difference of the roughness values, and that behavior is similar before and after being abraded surfaces. However, the average values of the roughness of the coatings 88HV and 7525 have no statistically significant difference between them. Compared individually roughness values of the coatings, shows that there is a statistically significant difference between mean values of initial roughness and erosion of the eroded surfaces. A rough surface is more susceptible to erosion than a smooth surface. The surface roughness can also influence on the flow near the surface. The coating surface may also contain more binder than the rest of the material, especially after sintering. The binder is softer and easier to erode than the carbide particles. In as sprayed specimens with lower surface roughness the width and depth of the grooves were much smaller as compared to the grooves in those with higher surface roughness condition suggesting lower penetration in nanostructured coatings with high hardness.

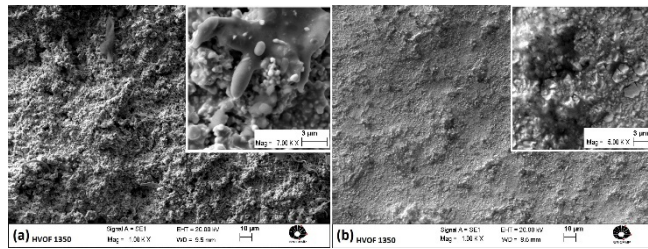


Figure 10. Images of scanning electron microscopy (SEM) of the original (a) and eroded surfaces (b) coating nanostructured 1350 VM / WC-731-1 in critical condition.

Source: Authors

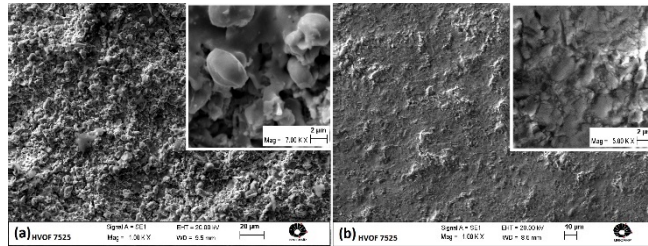


Figure 11. Images of scanning electron microscopy (SEM), (a) Original surface (a), (b) eroded surfaces of the conventional coating Cr3C2-NiCr 75-25 AMPERIT in critical condition.

Source: Authors

Images of scanning electron microscopy on Figs. 10 and 11 present at the critical conditions ( $V=9.33$  m/s,  $\alpha=90^\circ$ ) the surface coating of tungsten carbide (1350) and chromium carbide (7525) which showed the best and worst performance respectively. It can be seen clearly the variation of surface roughness before and after erosion. The analysis concluded that the decrease of the surface roughness in the coating tungsten carbide was 45.48% and a in the case of chromium carbide coating of 77.5%, being a factor in this behavior the value of microhardness of the coatings surfaces, which when greater causes less loss of roughness [14,15,25].

High magnification images of Figs. 10 and 11 details defects and damage shown on the surfaces of the coatings caused by erosion as: fractured zones, formation of multiple cracks, individual carbide particle removal exposing the soft metallic binder for erodent particles impacts creating the voids at their original sites where these carbides were, broken carbides grains, craters, etc.

Figures show that the mechanism of material removal in both coatings was due to the appearance of microcracks and caused by the repetitive impact of solid particles in a given region cracks, which propagate and cause the extrusion of the carbides reinforcement of the binder matrix, characteristic mechanism of brittle materials. In literature related to this topic similar behaviors can be found [1,10].

In coatings with conventional grain sizes it was observed that the increase rate of erosion is associated with lower hardness and lower fracture toughness. In the above figure shows a higher degree of plastic deformation as under its lower fracture toughness develop and grow cracks in its wake cause the extrusion of carbides grains, exposing the soft phase matrix with the repetitive impact of the erosive particles increases wear. Evidence was found from wear scar that some erosion damage can be localized at large pores, or isolated porous areas in 88HV

and 7525 NiCr coatings. As a consequence to repetitive high energetic impacts of erodent particles, cracking occurs over the coated surface, and with the course of time, these cracks have been grown up and propagated into radial and lateral cracks. At the junction of these radial and lateral cracks WC grain get loosened and came out of the surface leaving a visible void or pit as shown on Fig. 11.

Meanwhile the material made from nanostructured powders has a less consistent plastic deformation and coating erosion took place from few sites and it is mainly due to the chipping of WC grain and ploughing of soft metallic binder. The coating surface is not heavily eroded, some shallow pits are clearly visible and minor pullout of WC grain confirms the better erosion resistance. Nanostructured coating possess higher fracture toughness value, which had suppressed the nucleation and propagation of cracks formed by repeated impacts of erodent particles. Fig. 10 shows the crack propagation restriction near fine WC grains and which may have taken place to high fracture toughness offered by nanostructured phase. Due to high fracture toughness and hardness value the cracking followed by the pullout of WC grain is suppressed in nanostructured coating.

### 3. Conclusions

1. The samples coated with nanostructured powders (1350 VM / WC-731-1) had the highest microhardness value, lower porosity, higher fracture toughness and lower roughness, playing a key role in a low erosion wear. All these improvements are related with size powder particles, the density of the coating and the more uniform reinforcement carbides (WC) distribution.
2. The speed and angle of impingement of the solid particles in the mixture influences the behavior of the wear resistance, this can be attributed to the fact that with increasing speed of the particles, have more kinetic energy causing further damage on the coating surface in correspondence with the relative material hardness and erosive particle. Thus the experimental condition of greater value speed (9.33 m / s) and impact angle of  $90^\circ$  was defined as the most critical, where all coatings experienced the greatest value of the ratio of erosive wear, more AMPERIT incidence coatings Cr3C2-NiCr 75-25 and Colmonoy 88HV.
3. With the analysis of scanning electron microscopy of the coating surfaces was observed that the mechanism of material removal in the coatings was caused by fatigue of the product of repetitive impacts of the solid particles surface at a given site, causing the formation of microcracks, cracks and the spread of these. These processes promote loss of adhesion of carbide reinforcements to the binder matrix and extrusion of them, favoring the coating higher ratio of microhardness of the deposit with respect to the hardness of the abrasive, greater fracture toughness, denser structure and less porosity.

### References

- [1] Lalit T., Arora, N., Jayaganthan, R. Sood, R., An investigation on erosion behavior of HVOF sprayed WC-CoCr coatings. Applied Surface Science 258(3), pp 1225-1234, 2011. DOI: 10.1016/j.apsusc.2011.09.079



- [2] Sheng, H. et al., Cavitation erosion behavior and mechanism of HVOF Sprayed WC-10Co-4Cr coating in 3.5 wt% NaCl solution. *Trans Indian Inst Met*, 68(1), pp. 151-159, 2015. DOI: 10.1007/s12666-014-0440-5
- [3] Richert, M.V. et al., Microstructure characterization of chromium carbides coatings deposited by thermal spraying processes. *Journal of Achievements in Material and Manufacturing Engineering*, 55(1), pp. 108-112, 2012.
- [4] Souza, D. and Neville, A., Aspects of microstructure on the synergy and overall material loss of thermal spray coatings in erosion-corrosion environments. *Wear*, 263, pp. 339-346, 2007. DOI: 10.1016/j.wear.2007.01.071
- [5] Wang, L. et al., Effects of Cr on microstructure and hardness of HVOF-sprayed WC-Co coating. *Advanced Materials Research*, (317-319), pp. 301-306, 2011. DOI: 10.4028/www.scientific.net/AMR.317-319.301. DOI: 10.4028/www.scientific.net/AMR.346.301
- [6] Suresh-Babu, P. et al. The influence of erodent hardness on the erosion behavior of detonation sprayed WC-12Co coatings. *Wear*, 270, pp. 903-913, 2011. DOI: 10.1016/j.wear.2011.02.019
- [7] Lopez-Cantera, E. and Mellor, B.G., Fracture toughness and crack morphologies in eroded WC-Co-Cr thermally sprayed coatings. *Materials Letters*, 37, pp. 201-210, 1998. DOI: 10.1016/S0167-577X(98)00092-5
- [8] Xu, J. et al., Erosion-corrosion behavior of nano-particle-reinforced Ni matrix composite alloying layer by duplex surface treatment in aqueous slurry environment. *Corrosion Science*, 51, pp. 1055-1068, 2009. DOI: 10.1016/j.corsci.2009.02.029
- [9] Lima, C.R.C., Libardi, R., Camargo, F., Fals, H.C. and Ferraresi, V.A., Assessment of abrasive wear of nanostructured WC-Co and Fe-Based coatings applied by HP-HVOF, flame, and wire arc spray. *Journal of Thermal Spray Technology*, 23(7), pp. 1097-1104, 2014. DOI: 10.1007/s11666-014-0101-6
- [10] Thakur, L. AND Arora, N., A comparative study on slurry and dry erosion behavior of HVOF sprayed WC-CoCr coatings. *Wear*, 303, pp. 405-411, 2013. DOI: 10.1016/j.wear.2013.03.028
- [11] Allen, C. et al., The wear of ultrafine WC-Co hard metals. *Wear*, 250, pp. 604-610, 2001. DOI: 10.1016/S0043-1648(01)00667-6
- [12] Saha, G.C. et al., Erosion-corrosion resistance of microcrystalline and near-nanocrystalline WC-17Co high velocity oxy-fuel thermal spray coatings. *Corrosion Science*, 53, pp. 2106-2114, 2011. DOI: 10.1016/j.corsci.2011.02.028
- [13] Hawthorne, H.M. et al., Comparison of slurry and dry erosion behaviour of some HVOF thermal sprayed coatings. *Wear*, (225-229), pp. 825-834, 1999. DOI: 10.1016/S0043-1648(99)00034-4
- [14] Lima, C.R.C., Fals, H.C. and Sagaro, R., Developing alternative coatings for repair and restoration of pumps for caustic liquor transportation in the aluminum and nickel industry. *Surface & Coatings Technology*, 268, pp. 123-133, 2015. DOI: 10.1016/j.surfcoat.2014.08.010
- [15] Reyes-Mojena, M., Lima, C.R.C., Sagaro, R. and Fals, H.C., Tribocorrosion behaviour of cemented carbide coatings obtained by high velocity oxygen fuel spraying. *Int. J. Surface Science and Engineering*, 9(6), pp. 561-573, 2015. DOI: 10.1504/IJSURFSE.2015.072835
- [16] Grewal, H.S. et al., Identifying erosion mechanism: A novel approach. *Tribol Lett*, 51, pp. 1-7, 2013. DOI: 10.1007/s11249-013-0156-4.
- [17] Sundararajan, G. et al., Erosion efficiency-a new parameter to characterize the dominant erosion micromechanism. *Wear*, 140, pp. 369-381, 1990. DOI: 10.1016/0043-1648(90)90096-S
- [18] Richert, M. et al., The effect of chemical composition and thermal sprayed method on the chromium and tungsten carbides coatings microstructure. *Journal of Surface Engineered Materials and Advanced Technology*, 3, pp. 1-5, 2013. DOI: 10.4236/jsemat.2013.31001
- [19] Gandhi, B.K., Singh, S.N. and Seshadri, V., A study on the effect of surface orientation on erosion wear of flat specimens moving in a solid-liquid suspension. *Wear*, 254, pp. 1233-1238, 2003. DOI: 10.1016/S0043-1648(03)00109-1
- [20] Hussainova, I., Kubarsepp, J. and Pirso, J., Mechanical properties and features of erosion of cermets. *Wear*, 250, pp. 818-825, 2001. DOI: 10.1016/S0043-1648(01)00737-2
- [21] Hussainova, I., Microstructure and erosive wear in ceramic-based composites. *Wear*, 258, pp. 357-365, 2005. DOI: 10.1016/j.wear.2004.01.024
- [22] Wayne, S.F. and Sampath, S., Structure/ property relationships in sintered and thermally sprayed WC-Co. *J. Thermal Spray Technol.*, 1(4), pp. 307-315, 1992. DOI: 10.1007/BF02647158
- [23] Barber, J., Mellor, B.G. and Wood, R.J.K., The development of sub-surface damage during high energy solid particle erosion of a thermally sprayed WC-Co-Cr coating. *Wear*, 259, pp. 125-134, 2005. DOI: 10.1016/j.wear.2005.02.008
- [24] Santana, Y.Y. et al., Influence of mechanical properties of tungsten carbide-cobalt thermal spray coatings on their solid particle erosion behavior. *Surface Engineering*, 28(4), pp. 237-243, 2012. DOI: 10.1179/1743294411Y.0000000016
- [25] Bjordal, M., Bardal, E., Rogne, T. and Eggen, T.G., Erosion and corrosion properties of WC coatings and duplex stainless steel in sand-containing synthetic sea water. *Wear*, (186-187), pp. 508-514, 1995. DOI: 10.1016/0043-1648(95)07148-2

**M.A. Reyes-Mojena**, is a full time professor in the Department of Mechanical Engineering of the University of Oriente, Cuba. He received his MSc. in Reliability and Maintenance from the State University of Campinas, Brazil. He is a PhD student at University of Oriente and his current research interests include hardfacing, thermal spray and Tribology. He earned a Sciences Academic Annual Award of Cuban Republic with the research "Influence of microstructure of cemented carbides in damage tolerance induced under service conditions" in 2015.  
ORCID ID: 0000-0001-5101-1998

**M. Sánchez-Orozco**, is a full time professor in the Department of Mechanical Engineering, University of Oriente, Cuba. He received his PhD on Technical Sciences in 2014 and Postdoctoral studies at the Federal University of Uberlandia, Brazil. He earned a Sciences Academic Annual Award of Cuban Republic in 2015 with the research "Influence of microstructure of cemented carbides in damage tolerance induced under service conditions". His current research interests include welding process characterization and surface engineering and coatings.  
ORCID ID: 0000-0003-1390-9582

**R. Sagaró-Zamora**, is a full time professor in the Department of Mechanical Engineering, University of Oriente, Cuba. He received his PhD on Tribology in 1995 and Post doctorate studies in Brazilian universities of Uberlandia and Piracicaba. He earned a Sciences Academic Annual Award of Cuban Republic in 1990 with the research 'Tribological behavior of composite materials for railway brake cars' and in 2015 with the research "Influence of microstructure of cemented carbides in damage tolerance induced under service conditions". He has authored more than 60 papers in journals and conferences. His current research interests include, surface engineering, nanocoatings, biomechanics and Tribology.  
ORCID ID: 0000-0001-5808-1999.

**H.D. Carvajal-Fals**, is a full professor at the Materials and Manufacture Department, at the University de Oriente, Cuba. He received his PhD on Mechanical Eng. from the State University of Campinas and made postdoctoral study in National Institute of Sincrotron Light in Campinas (ABTLuz), SP, Brazil. His current research interests include welding metallurgy and process, surface engineering and coatings. He earned a Sciences Academic Annual Award of Cuban Republic with the research "Influence of microstructure of cemented carbides in damage tolerance induced under service conditions".  
ORCID ID: 0000-0001-5061-8763

**C.R. Camello-Lima**, is titular professor at UNIMEP – Methodist University of Piracicaba, SP, Brazil. He has more than 100 articles published in journals and international conferences. He received his MSc. and PhD. in Mechanical Eng. from UNICAMP – State University of Campinas, São Paulo, Brazil. He is a visiting professor in the CTSR, Center for Thermal Spray Research – Stony Brook, NY, USA (1998–1999) and also at Thermal Spray Center, University of Barcelona, Spain (2004–2005). He has 20 years of industrial experience in industrial maintenance and metallurgical processes.  
ORCID ID: 0000-0002-7669-4059.